Observing Sea Surface Salinity in Coastal Domains Using an Airborne Surface Salinity Mapper

Derek Burrage[1], Jerry Miller[2], Don Johnson[2], Joel Wesson[2] and Jeff Johnson[1]

[1]Dept. of Marine Science, Univ. of Southern Mississippi, Stennis Space Center, MS, 39529, USA.

derek.burrage@usm.edu,

[2] US Naval Research Laboratory (NRL), Ocean Sciences Branch, Stennis Space Center, MS 39529, USA.

***Abstract*- Sea Surface Salinity directly affects the status of coastal ecosystems and serves as a tracer for seawater constituents associated with freshwater runoff. As part of an NRL-sponsored study of the dynamics of coastal buoyancy jets (CoJet), which began in July, 2000, the original Scanning Low Frequency Microwave Radiometer (SLFMR) was deployed in various coastal locations to evaluate its performance for mapping sea surface salinity, and demonstrate its application to studies of coastal plumes and buoyant jets. In a sequence of three campaigns, the radiometer was flown repeatedly over the Cheseapeake and Mobile Bay plumes and over the northern Gulf of Mexico and Florida Bay using a twin-engine Piper Navajo aircraft. Extensive surveys of sea surface salinity distributions were conducted on time scales of a few hours. The instrument was field calibrated using in situ data from oceanographic research vessels and the resulting salinity maps were corrected for known environmental influences. The logistical convenience and broad dynamic range of the instrument allowed surface maps to be generated quickly over waters that were either significantly fresher or more saline than standard seawater. The instrument performance and resulting map quality were thus found to meet the requirements of coastal oceanographic studies that are characterized by large buoyancy signals, and a variety of forcing effects that evolve relatively rapidly in time and space. The instrument and data processing system are first described and two new methods of field calibration method are presented. Examples of surface salinity maps of rapidly evolving coastal plume features are then described and interpreted using supporting in situ data. Finally, the overall capability and utility of the system is evaluated, and recent advances in the technology and future prospects are briefly considered.**

I. INTRODUCTION

Sea Surface Salinity (SSS), or salt concentration, is a key property of marine waters that directly affects the physical and chemical environment, health and status of coastal ecosystems. It also serves as a tracer for other sea water constituents, such as sediments, nutrients and pollutants which may be associated with freshwater runoff. The development of microwave remote sensing capabilities in the later half of the 20th century [1] resulted in the first airborne observations of SSS in 1970 in transects over the Mississippi River outflow [2]. The original Scanning Low Frequency Microwave Radiometer (SLFMR), developed for NOAA by Quadrant Engineering Inc. (now ProSensing Inc.) has been deployed in a number of estuaries and the continental shelve waters off the US East and South East coast [3,4, 5]. Beginning in July, 2000, it was deployed in an NRL-sponsored study of coastal buoyancy jets (CoJet). The purpose of this paper is to describe a novel method developed to field calibrate this instrument and to present indicative results obtained from the CoJet flights over Florida Bay, off Cheseapeake Bay and in the northern Gulf of Mexico.

Calibration and deployment of a second SLFMR built in 1999 for an Australian research consortium are described elsewhere in these proceedings [6, 7]. That instrument has been flown extensively to map tropical river plumes in the Great Barrier Reef Lagoon during three experiments conducted in the period 2000-2002 "in press" [8],[9, 10].

The purpose of the NRL CoJet deployments was to evaluate the performance of the SLFMR for mapping SSS, and to demonstrate its application to multi-disciplinary studies of coastal plumes and buoyant jets. In a series of four experiments using a suitably outfitted twin-engine Piper Navajo Chieftain charter aircraft, the radiometer was flown repeatedly over the Chesapeake Bay entrance and adjoining continental shelf, over Mobile Bay and adjoining Mississippi Sound and northern Gulf of Mexico, and over Florida Bay (Table 1).

TABLE I
DATES AND LOCATIONS OF COJET EXPERIMENTS

Dates	Campaigns	
	Experiment	Location(s)
18-24 Jul 2000	CoJet-I	New Jersey Coast and Continental Shelf
12-22 Sep 2000	CoJet-II	Chesapeake Bay entrance and Continental Shelf
16-30 May 2001	CoJet-III-MS	Mobile Bay, Mississippi Sound and Northern Gulf of Mexico
02-05 Jun 2001	CoJet-III-FB	Florida Bay

Using the system, extensive surveys of SSS distributions were conducted on time scales of a few hours. The instrument was field calibrated using a novel approach, utilizing sea-truth data from coastal research vessels. The resulting salinity maps were corrected for known environmental influences. The accuracy, precision and spatial resolution of the maps were found to be well-matched to the requirements of coastal oceanographic

studies, which are characterized by a variety of forcing effects that evolve relatively rapidly in time and space.

We first describe the instrument, data acquisition and processing (Section II) and method of field calibration (III). The capability of the salinity mapping system is then illustrated by examples showing coastal buoyancy features and transient changes observed over several day periods (IV). The overall capability and utility of the system is evaluated based on our accumulated experience, and recent advances in the technology are briefly discussed (V) before general conclusions are drawn (VI).

II. THE SALINITY MAPPING SYSTEM

A. The SLFMR

The Scanning Low Frequency Microwave Radiometer comprises a single channel L-band microwave radiometer that sequentially observes microwave brightness temperatures through an 8-channel beam forming matrix and antenna system [1]. The radiometer is a thermally-regulated Dicke Radiometer design with a null feedback loop [11,12]. This design minimizes the effects of receiver noise, drift due to amplifier gain variations, and transients caused by operating temperature variations [13,1]. With the antenna mounted underneath the aircraft fuselage, the beams point downward and to either side of the aircraft at nominal angles of incidence of +/- 7, 22, 37 and 50 deg with respect to the vertical (nadir). Due to poor side-lobe response, the outer beams are not used. The remaining beams are denoted from left to right across the scan 3L, 2L, 1L, 1R, 2R and 3R. Half-power beam widths are nominally 15 deg. At typical flight altitudes of 2600m this gives a footprint that is 700m wide near nadir and increases with incidence angle. The beams, which are multiplexed through a single radiometer assembly, are poled sequentially at 0.5 sec intervals in a 'fly-back' scanning mode [13] so that a single across-track scan takes about 4 sec. At typical aircraft speeds this allows an area of about 60 x 60 km to be mapped at a nominal spatial resolution of 1km in about 4 hours [8]. The instrument includes a GPS navigation system and gyros giving precise time, position (lat, long) and orientation (pitch, roll). The instrument operates in the L-band at a frequency of 1.4 GHz with a bandwidth of 25 MHz. At this frequency the depth of penetration in seawater is of order 6 cm. The band falls intentionally within a protected, hence 'quiet', portion of the EM spectrum that is allocated for astronomical observations. Nevertheless, out of band radio frequency interference (RFI) thought to originate from active radar systems operating near certain large cities, as well as in-flight radio communications, can be problematic. Within this band, the electrical conductivity, and hence emissivity of the sea surface is a strong function of sea surface temperature (SST) and salinity [14]. If SST is known, the brightness temperature of the natural sea surface emission can thus be inverted to deduce the sea surface salinity. To accommodate this, the SLFMR is flown with a companion nadir-viewing dual channel infrared radiometer system to observe SST. The SLFMR was constructed by Quadrant Engineering (now ProSensing) of Amherst, MA in 1990 and subsequently was tested extensively during flights conducted by NRL in cooperation with NOAA. It was used to obtain the world's first airborne sea surface salinity map over the Chesapeake Bay entrance during the Coastal Ocean Processes Experiment (3,4), and was therefore at an advanced stage of development when CoJet operations were commenced in the year 2000.

B. Data Acquisition and Processing

During in-flight operation, data are acquired simultaneously from the SLFMR and companion Infrared radiometer system and are logged on a computer hard-disk. The dedicated computer displays the resulting brightness temperatures and ancillary data in real time, allowing the operator to monitor and verify instrument performance, and advise the pilot if flight track adjustments are required. Post-flight processing is done using a custom computer processing system (RADOS) developed at NRL using MATLAB (The Mathworks, Inc.). This system is largely automated. RADOS comprises a suite of modules and standardized data structures that facilitate semi-automated data editing and correction for environmental influences using a variety of theoretical and empirical algorithms [13, 15]. After data are converted to geophysical values they are checked for anomalies due to such factors as locally-generated instrument noise, RFI and sudden attitude changes, and corresponding data spikes are eliminated. The remaining data are interpolated and filtered as required. Infrared data are checked for cloud contamination and affected data are removed. A dual window water vapor correction is then applied to produce calibrated *SST* values. The L-band brightness temperature data are similarly treated and anomalous high values due to the appearance of land in the field of view are removed. Once editing is completed a number of environmental corrections are applied. Reflected microwave O_2 emission originating from the atmosphere above and below the aircraft is estimated and subtracted from the raw L-band brightness temperatures. Nominal corrections are also applied for the reflected extra-terrestrial emissions from the microwave background radiation (due to the 'big bang') and from the Milky Way Galaxy. These are estimated using tabulated astronomical H_2 line and continuous spectral data acquired within the 1.4 GHz band. The effects of much stronger reflected solar emissions ('sunglint') can be detected by inspection, since brightness temperatures are biased consistently high in the up-sun direction. The effects of sunglint are more severe under rough sea conditions due to diffuse surface scattering from the ocean surface. Since corrections for sunglint are not yet available, it is usually avoided by flying near dawn or dusk. Corrections for enhanced emission due to atmospheric water vapor and sea surface roughness, which is mainly a function of wind speed, are optionally applied. If necessary, additional iterations in the editing and correction process can be carried out before calibration. 'Quicklook' raw data graphs and images can be produced almost immediately. At this stage, a preliminary

calibration procedure that uses a beam equalization process and/or application of representative regional salinity values can also be applied. Final fully-calibrated products can be produced once shipboard in situ data become available.

III. CALIBRATION

Application of L-band radiometry to salinity mapping demands exceptional sensitivity and high accuracy, both of which involve tradeoffs in such factors as antenna design and selection of operating band width, and sampling rates. Sensitivities of ~ 0.5 K, which are required for a corresponding salinity resolution of about 1 psu are theoretically attainable with existing radiometer designs, but difficult to achieve in practice, when total system performance is taken into account.

Modern designs have led to very significant advances in sensitivity (precision) and stability (accuracy), as well as immunity to external and internal thermal and electromagnetic disturbance. Despite these advances, the stringent demands and complexities imposed by the physics of SSS retrieval dictate that careful attention be paid to calibration both in the lab and in the field, if satisfactory results are to be obtained. For example, noticeable 'image striping' artifacts can appear in the resulting SSS maps, even when beam-to-beam differences in the accuracy of the brightness temperature measurement are relatively small.

A. Laboratory Calibration

Full laboratory calibration of a microwave radiometer requires at least two stable targets with accurately known brightness temperatures spanning the required instrument range (nominally 50 to 350 degrees Kelvin with typical land and sea values being 300 and 130, depending on incidence angle, and the effective emissivity of the surface). A target for the high end of the range is readily attained by monitoring the physical temperature of microwave absorbing material surrounding the instrument, at ambient room temperatures. The low end of the range requires cryogenic cooling of microwave absorber material, which is difficult to achieve in practice due to 'icing' and other complications. An alternative cold target selected for 'lab' calibration of the SLFMR was the night sky which radiates close to the microwave background level of ~3K, plus a contribution due to atmospheric O_2 (~5K), giving a total target brightness temperature of ~8K. The possible effects of Galactic emissions were not fully appreciated, nor accounted for, in early lab calibrations of the SLFMR.

The procedure (Mark Goodberlet, ProSensing unpublished notes) involved alternately pointing the antenna beams to the night sky and towards microwave absorber at a known ambient temperature, while warming then cooling the instrument through its operating temperature range. A multiple regression procedure [16] was then used to deduce calibration coefficients for apparent brightness temperature as a function of the target temperature and internal instrument temperatures. Since details of such procedures are available elsewhere in these proceedings [6], they are not discussed here. In spite of these efforts, experience during the COPE flights showed field calibration was also required to obtain accurate salinity retrievals. This was done by comparing in situ surface salinity observations with coincident salinities retrieved from the SLFMR using the manufacturer's calibration coefficients. A Salinity offset was applied to align the SLFMR observations with the in situ observations 'in the mean'. This procedure is satisfactory only if the airborne survey salinity values do not vary widely, since the brightness temperature versus salinity relationship, which is given by the well-established Klein and Swift (K&S) algorithm [14] is inherently non-linear. The field calibration methods developed for CoJet and described next, overcome this limitation.

B. Preliminary Field Calibration

This method involves two related steps viz. assignment of a 'first guess' mean salinity value and beam equalization. It operates by adjusting the brightness temperatures because this what is measured by the radiometer, rather than the salinities, which are derived from them using the K&S algorithm. Thus, in contrast to the Salinity offset approach, the method fully accounts for non-linearities in the *SSS* retrieval algorithms.

The method is useful if there are insufficient field data to calibrate beams individually, or if only climatic or typical values of salinity for the survey region are known from previous observations. It is also useful for creating preliminary maps, before the full in situ data set becomes available. Beam equalization is used to eliminate beam-to-beam differences in brightness temperature calibration offset, which manifests as a image striping artifacts.

A representative salinity value is first chosen for the region. This could be a 'wild guess' if no prior information exists, a 'best guess' based on a spatially-averaged value of the region obtained from historical data or a climatology, or a preliminary value derived from the available ship data obtained at the time of the survey. This initial SSS value, along with a corresponding 'first guess' SST is used to compute apparent brightness temperatures for each beam under the survey flight (e.g. aircraft altitude, attitude bias, and beam incidence angle). Simply using the K&S algorithm to obtain the corresponding brightness temperature (T_B) that would be observed by a nadir-viewing instrument just above the sea surface is not sufficient. Rather, the incidence angle dependence and effect of the intervening atmosphere (reflected O_2 emission), must be taken into account to obtain a 'predicted' apparent brightness temperature value (T_A') comparable with that sensed by the radiometer mounted on the aircraft (T_A).

Beam equalization now proceeds by determining the mean apparent brightness temperature ($\langle T_A^k \rangle$) observed by the k'th beam over the survey domain and comparing this with (T_A') derived from the first guess SSS and SST values. The differences $T_A' - \langle T_A^k \rangle$ for each beam are then used to add a brightness temperature offset to all the data acquired using that beam. Future calculations based on the adjusted

brightness temperatures T_A will now yield the same salinity values in the mean for each beam, thus minimizing striping and yielding realistic salinity values that will be correct within the error of the 'first guess' salinity. The maps produced by the preliminary calibration are useful for evaluating relative point to point salinity changes, frontal contrasts and spatial gradients, even though the absolute salinity values may be unknown.

The key assumptions of the method are: i) the 'first guess' SST and SSS are representative of the region, or at least 'valid' in the sense that they are within the range of the K&S algorithm, ii) the mean salinity retrieved from all the beams over the survey domain do not differ significantly and iii) the T_A calibration error may be accounted for by a simple offset, which implies that the regression slope coefficients determined from lab calibration have not changed significantly. Assumption i) is easily met and needs no further justification. Assumption ii) will be met when a significant fraction of the survey senses a relatively homogenous ocean surface, and/or when the aircraft crosses frontal features without an overall strong bias toward higher salinities one side of the aircraft or the other. Conventional flight patterns usually conform to these requirements, but unusual flight patterns where, for example, the aircraft flies along a frontal line or closely parallel to a buoyant coastal current for most of the survey would violate the assumption. Assumption iii) is supported by repeated lab calibrations which show that while the offset may very significantly, the regression slopes generally do not (M. Goodberlet, personal communication). However, the results of recent field calibrations suggest this requires further investigation. There are also practical difficulties obtaining a stable multiple regression result, due to multi-colinearity in the input variables, which may cause this assumption to be violated. The SLFMR housing contains thermal regulators maintaining various instrument components at a uniform operating temperature (typically 40 C) that cannot be individually switched off and on. As a consequence, during instrument warm-up and cool-down, the component temperatures strongly co-vary, so that a wide scatter of independent variable values cannot readily be obtained for the regression [6].

C. *Final Calibration*

Final calibration can be applied when sufficient in situ field data are available to allow beams to be individually calibrated. If this not the case, then the preliminary calibration procedure can be applied using a mean value applicable for the survey as a more precise input than a simple 'first guess'. Final calibration uses 'valid' SLFMR salinity values obtained by preliminary calibration as a starting point for comparisons with in situ data. The radiometer and in situ data are scanned to find matching data sets falling within a representative spatial and temporal search radius. The matching variables are ship and SLFMR beam footprint position on the sea surface and the time of observation. Typical search radii are 1km and 1 hr, respectively. However, larger search radii can be used if the regional salinity varies relatively slowly in space or time. Matched pairs for each beam are accumulated over the survey area and apparent brightness temperatures, T_A', corresponding to the in situ *SST* and *SSS* are computed using the K&S algorithm as in the preliminary calibration, but stored separately for each beam. Individual T_A offsets are then computed from ship and radiometer mean values for each beam. These are applied to each beam as a final calibration correction. It is theoretically possible to perform field calibration by computing multiple regression slope coefficients for the individual beams, taking into account the instruments internal temperatures, in addition to a simple T_A offset. However, it is practically impossible to acquire enough in situ data over adequate operating temperature spans to give a reliable multiple regression. Instead, simple linear regression between the T_A and T_A' pairs is carried out, and the resulting regression slopes and R^2 values are used as a check on the quality of the fit. Standard errors can be assigned to the mean offset and slope coefficients as an objective indicator of the quality of the calibrated image products. A similar regression procedure can be applied to the retrieved salinities derived from the calibrated T_B values and corresponding in situ salinities.

The SSS maps shown in this paper were all produced using the preliminary calibration procedure with a spatially-averaged salinity obtained from all the available in situ data spanning each flight sequence. Brightness temperature offsets obtained with this method, which utilizes beam equalization, are compared with the offsets obtained from the final calibration method which compares in situ data directly with data from individual beams (Table 2).

TABLE II
PERFORMANCE OF PRELIMINARY AND FINAL CALIBRATION FOR SELECTED COJET CAMPAIGN DATA

Exp. / Flight Date	Salinity Fit R^2, Slope, a r,Resid sdv		Beam T_B [K] Offsets for Preliminary (upper) and Final Calibration (center,bold). Beam T_B Preliminary Standard Deviation (lower)					
	R^2 r	a.	3L	2L	1L	1R	2R	3R
Manuf. Calib. (**79.9**)			**1.2**	**13.5**	**-8.0**	**-1.7**	**-13.8**	**8.8**
II 9/17 (**99.6**)	**0.18** 6.9	**0.64**	3.2 **3.4** 2.5	0.9 **1.5** 2.0	-12.3 **-12.3** 1.9	0.1 **0.4** 2.2	3.0 **3.0** 2.2	5.1 **4.1** 2.6
III-MS 5/17 (**84.2**)	**0.30** 9.3	**0.45**	0.2 **1.7** 3.9	1.70. **0.6** 3.2	-7.7 **-9.1** 3.2	2.0 **1.8** 3.2	3.4 **3.4** 3.1	0.5 **0.8** 3.3
III-FB 7/02 (**88.4**)	**0.84** 2.5	**0.90**	1.5 **-1.4** 16.0	0.9 **2.4** 9.6	-9.6 **-6.9** 5.0	1.5 **2.7** 6.3	2.0 **1.4** 7.4	3.6 **1.7** 8.4

Table entries are goodness of fit, R^2 (bolded), residual standard deviation, r (unbolded, col 1.) and regression slope coefficient, a (col 2), for remotely-sensed versus in situ salinities for the final calibration (combining all

beams). Entries in column 4-9 give corresponding brightness temperature beam offset statistics as follows: The bolded (center) entries are T_B offsets derived using the final calibration method. The unbolded entries in each cell are beam T_B offsets deduced from the preliminary calibration method for the given flight date (upper entries) and standard deviations of all the measurements from each beam for that flight (lower). The mean of the final calibration T_B offsets for all six beams was subtracted from both the preliminary and final entries before tabulation to give an indication of relative beam differences. The mean offsets, which indicate how much the instrument calibration deviates from the initial CoJet lab calibration (first row), were 19.7, 4.3 and 8.46 K for Experiments II, III-MS and III-FB, respectively. The actual mean calibration offset (or regression intercept) is shown in parentheses (bolded) in column 1.

Changes in these means and the relative (bolded) T_B offsets from experiment to experiment give an indication of the calibration drift of each beam. Differences between the unbolded and bolded offsets (cols 4-9) provide a retrospective measure of the accuracy of the preliminary calibration, while the standard deviation indicates the combined effect of instrument and sampling noise. Errors in the preliminary calibration can be significant, ~ 2 K, but are generally below the noise level (~ 5 K, depending upon beam) for the SLFMR. This relatively high noise level applies to point to point 0.5s samples acquired at intervals of about 4s. The level can be lowered significantly by averaging at the expense of reduced spatial resolution. The maps shown here were averaged along-track (but not across beams) using a 3km box car filter (2km for CoJet-II).

D. Field Calibration Results

The last laboratory calibration performed on the NOAA SLFMR prior to commencement of the CoJet experiments was carried out in Dec, 1997. The regression offsets for this calibration were adjusted by the manufacturer using field data from a Florida Bay survey conducted on 5 Feb, 1998. The mean offset (regression intercept) was 79.9 K (see Table 2 for the relative beam deviations from this mean), while offsets for each experiment were 10-20 K higher. This suggests that to obtain accurate survey results without extensive field calibration, lab calibrations should be performed at least before and after each series of flights, and preferably before each flight. Early experience with field-calibration of the Australian-owned SLFMR indicates mean offsets can change during a particular experiment by about 1 K (~2 psu) from flight to flight [8, 6].

The best salinity regression fit, with high R^2, low residuals and slope close to unity, was obtained for the Florida Bay study, where a wide range of salinity values were sampled by both the aircraft and ship. In situ sampling during CoJet-II was confined mostly to the frontal domain, so the salinity range was more restricted and locational errors likely larger. We also suspect that outliers due to land contamination still remain in the CoJet III-MS data that could be removed with more sophisticated topographic editing.

Relative beam offsets also changed significantly. Initially 2L and 2R were highest and lowest, respectively among the beams, whereas 1L was anomalously low during CoJet-III. Clearly, changes in calibration can affect individual beams, which tends to implicate the antenna system or its environment since, in the SLFMR, the beams are multiplexed through a single Dicke radiometer assembly.

To illustrate the calibration procedure we give examples of regression plots for the Florida Bay flights conducted at the end of CoJet-III. A regression plot combining matches for all beams and both flights (Fig. 2.) shows that the airborne salinities explain 84% of the variance of the in situ data.

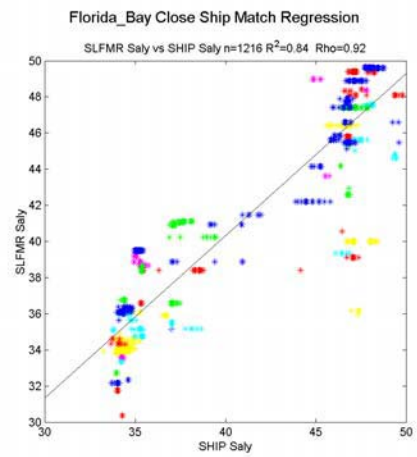

Fig. 1. SLFMR V's in situ SSS after preliminary calibration showing a correlation coefficient of 0.92 and regression slope of 0.89 and residual standard deviation of 2.5 psu. Beams 3L, 2L, 1L, 1R, 2R, 3R are color coded yellow, magenta, cyan, red, green and blue respectively.

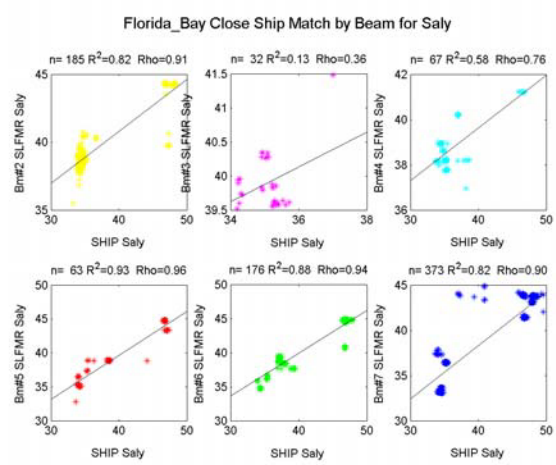

Fig. 2. Individual Beam V's in situ SSS after preliminary calibration showing a correlations exceeding 0.9 for 4 of the 6 beams. Poorer results for beams 2L and 1L reflect fewer matches and the effects of outliers due to proximity to land. Residual standard deviations vary from 10 to 20 psu.

Sea Surface Salinity fits for individual beams (Fig 2) showed significant scatter due to high T_B outliers. Because T_B is inversely related to SSS, these produce anomalously low salinities. Despite the application of filtering operations designed to detect and remove beam data acquired over land, some outliers remain where SLFMR beam spots fall near islands and shoals. Finer resolution topographic survey data and polygon land editing techniques will help address this problem. In the present data sets outliers were simply eliminated by excluding data falling beyond the 95 percentile of each channel. Despite these deficiencies the mean T_B offsets computed using the two methods were similar (Table 2).

IV. COJET SURVEYS

A. Mapping a Hypersaline plume – Florida Bay

Previous airborne salinity mapping over Florida Bay using the SLFMR demonstrated its utility in monitoring the distribution of freshwater inputs from the Florida Everglades during the wet season (June-October), when significant areas are occupied by low salinity waters [17]. However, instances of hypersaline conditions have been reported during the dry season, January-May.

The SLFMR was flown over Florida in the first week of June, 2001, effectively at the seasonal transition. The purpose of these flights was to determine the spatial extent of the high salinity plume that develops in an extensive shallow water region during periods of low rainfall and/or strong evaporation in the region. Although only a few flights were made, in situ SST and SSS data were simultaneously acquired from a boat-mounted salinograph (K. Chen, personal communication). The instrument was a Signet Inc. conductivity meter with an of accuracy of ± 1% and response time of 2 sec. Sample water was pumped from a depth of 20 cm. The resulting was used to field calibrate the SLFMR, and to effectively extrapolate the absolute in situ salinities to the flight survey domain.

Results shown for the morning flight on 2 June, 2001 (Fig. 3), were processed using the preliminary calibration procedure just described (section III, B) using the mean in situ salinity of 42.9 psu as a 'first guess'. The afternoon flight carried out from a lower altitude (not shown) produced a similar salinity distribution, even though SST's were about 2 deg C warmer. In the later flight, an initial transect from the SW showed the hypersaline zone extended all the way to 24.9 S and 80.9 W. The residual striping effect evident here could be due to sunglint or radio frequency interference (RFI) affecting beams 3L and 2L. It was much less noticeable in the late afternoon flight, perhaps because of lower sun angles, calmer seas and or reduced RFI, which may be blocked by the horizon at lower altitudes.

The retrieved salinities (Fig. 3) may be compared with the corresponding in situ data plots (Fig. 4). The in-situ salinity data and the two airborne surveys show the same region of maximum salinity in the very shallow waters (1-3 ft 0.3 -1m) in the central northern section of Florida Bay. The high salinity region is separated from the eastern section where there are many small rivers emptying into the Bay. The western section is fed only by Taylor Slough. The combination of very shallow passages from east to west, the lack of fresh water supply and excess evaporation result in exceptionally high salinity in the central section. In addition, the very shallow water keeps open ocean waters from diluting the high salinity waters. The pronounced hypersaline region present in central Florida Bay in June, 2001, also appears in salinity maps derived from in situ measurements [18] that show surface salinities exceeding 45 psu.

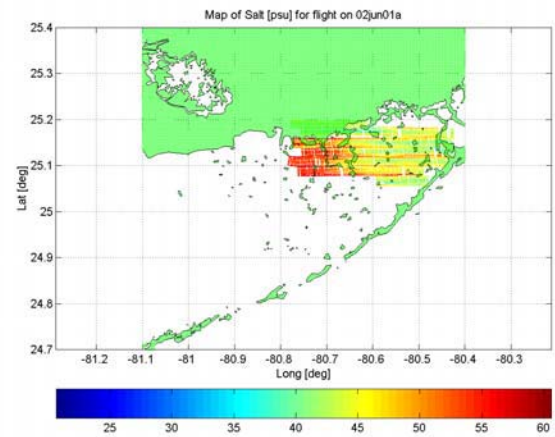

Fig. 3. SLFMR SSS map showing hypersaline conditions in Florida Bay exceeding 50 psu west of Long. 80.65deg W.

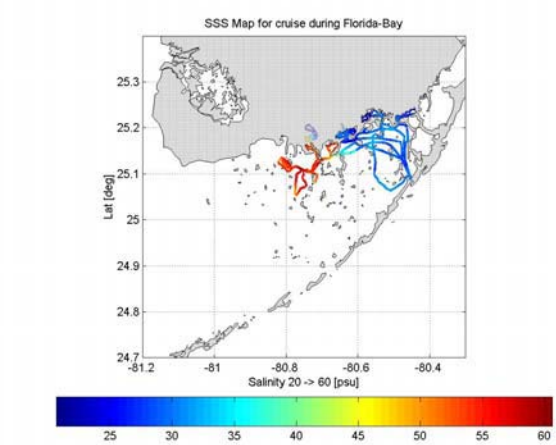

Fig. 4. Shipboard SSS map showing hypersaline conditions in Florida Bay exceeding about 50 psu west of Long. 80.65deg W.

The appearance of relatively sharp changes in salinity at similar locations in the in situ and airborne maps suggests that relative SSS changes are well represented by the SLFMR, even beyond the range of the original K&S algorithm (38 psu) [14]. This range was recently extended experimentally to 40 psu "unpublished" [19], but it appears that further extension to ~45 psu or higher might be possible. These hypesaline results, which are necessarily tentative, open up the possibility of using the SLFMR to

monitor changes in other hypersaline environments that are found elsewhere in the world (e.g., Shark Bay, Western Australia is a geologically-significant example of a hypersaline marine environment that supports modern stromatolite beds, previously found only in ancient reef deposits).

B. Upwelling in the Chesapeake Bay Outflow Plume

The SLFMR was previously flown over the entrance to Chesapeake Bay during the COPE experiment, during which significant plume development produced by high river runoff was observed [3,4]. During CoJet-II, six complete surveys were carried out over the entrance, along the adjoining coasts between latitudes 36 12' and 37 24' N and offshore to longitude 75 30' W. Within the period spanning the flights, 12-20 Sept., 2000, oceanographic data including near surface temperature, salinity and current observations were obtained from shipboard thermo-salinograph transects and from in situ moorings.

The representative SSS maps shown in Fig. 5 and 6 were produced using the preliminary calibration procedure with a mean salinity of 29 psu, obtained from all thermo-salinograph records spanning the experimental period within the area of interest. While the mean SLFMR salinity over the whole region on each flight is constrained to match this ship survey mean, the relative changes observed in each SLFMR map are independent of the shipboard data. The resulting brightness temperature offsets are compared with those obtained from the final calibration procedure in Table 2.

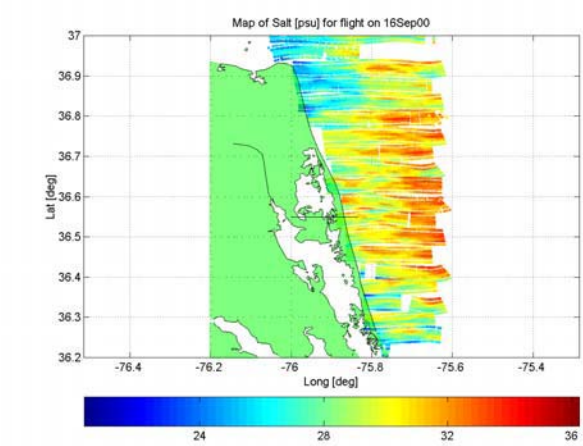

Fig. 5. SLFMR SSS map showing restricted development of the Chesapeake Bay outflow plume on 16 Sep, 2000. The image was acquired during downwelling favorable wind conditions.

The maps show little plume development south of the entrance on 16 Sept., but moderate plume development on 17 Sept. Objectively mapped data from the ship salinograph survey obtained within the 24 hr period separating the two flights (not shown) agreed closely with the airborne SSS map of Fig. 6. The airborne survey was conducted during a brief calm period within a transition from southward to northward-directed wind stress events reaching $0.2 Nm^{-2}$. During this transition period the alongshore currents within the plume changed from southward to northward with speeds of up to $0.25 ms^{-1}$. The wind relaxation process was thus consistent with a shift from downwelling to upwelling favorable conditions.

The map from the preceding flight on late 16 Sept. shows the plume confined to the coast south of the entrance, but by late 17 Sept. it had clearly expanded offshore. The remotely-sensed data shows a more southerly extension of the plume at this time. This extension appeared after the shipboard survey had been completed and was documented by subsequent ship observations. The remotely sensed SSS distributions are thus consistent with the observed upwelling response and southward extension of the plume originating from Chesapeake Bay.

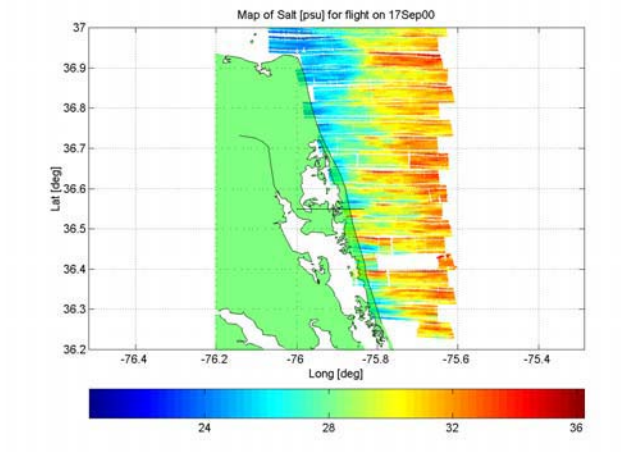

Fig. 6. SLFMR SSS map showing moderate development of the Chesapeake Bay outflow plume on 17 Sep, 2000. The image was acquired after relaxation of downwelling favorable winds.

C. Mobile Bay and the Gulf of Mexico

The first airborne SSS surveys over Mobile Bay, Mississippi Sound and the northern Gulf of Mexico were carried out with the SLFMR during CoJet-III. A total of 15 flights were completed over Mississippi Sound and the adjoining continental shelf (Table 1). Several flights ended with a transect north along the axis of Mobile Bay. Figs. 7 and 8 show the prevailing SSS distribution during a period of south-west winds (wind stress directed toward the NE). Turbidity maps derived from the satellite-borne SeaWIFS ocean color sensor show turbid water confined largely to Mobile Bay and Mississippi Sound, but with plumes of moderate turbidity southeast of the Mobile Bay entrance (not evident in the available airborne SSS map data) and in the vicinity of the Chandeleur Islands.

Figs. 9 and 10 show a distinctly modified SSS distribution with freshwater confined largely to Mississippi Sound and the area west of the Chandeleur Islands, with little plume development offshore. By this time the winds were mostly blowing from the north (southward directed wind stress), which would favor westward Ekman drift on the continental shelf. The Mobile Bay transect on the 22nd (Fig. 9) cuts across the Mobile Bay plume, which appears to be confined west of the entrance. The latter observation is confirmed by a coincident SeaWIFS image. Previous studies have shown that the Mobile Bay plume responds rapidly to wind stress in the Ekman sense, i.e. the plume

tends to expand to the right at right angles to the prevailing wind direction [20]. Changes in the larger-scale SSS distribution evident in the SSS maps appear to be consistent with this effect.

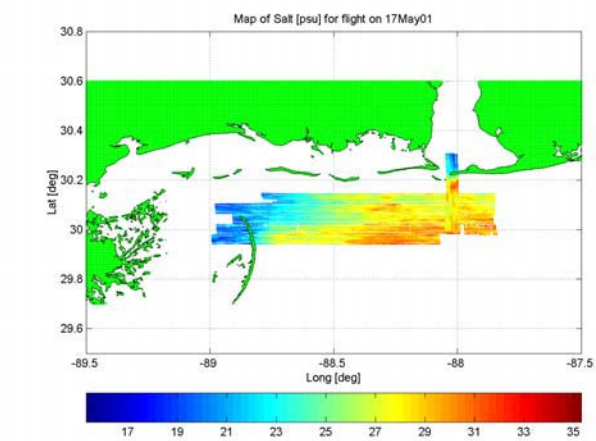

Fig. 7. SSS map showing Mobile Bay plume apparently restricted to the Bay and vicinity of Chandeleur Islands on 17 May, 2001.

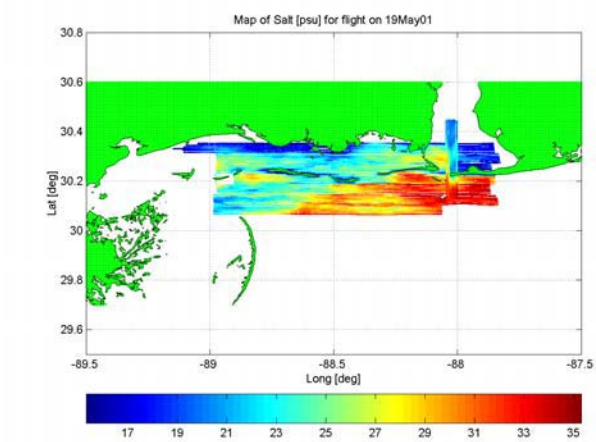

Fig. 8. SSS map from 19 May, 2001 showing the development of a salinity front running WSW of the entrance to Mobile Bay. A continuous body of fresher coastal water occupies Mississippi Sound. Prevailing north-eastward wind stress favored south-eastward expansion of the plume.

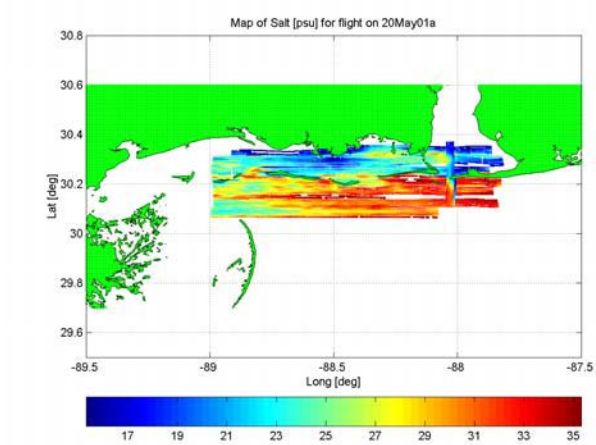

Fig. 9. SSS map showing the plume confined largely to Mobile Bay and Mississippi sound with restricted development offshore toward the west on 20 May, 2001.

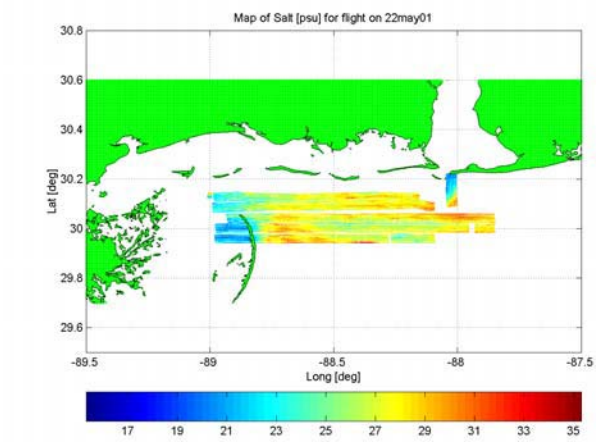

Fig. 10. SSS map from 22 May, 2001 showing restricted plume development, but with a body of freshwater emerging south of the Mobile Bay entrance. Wind stress, directed predominantly east-south-eastward, favored westward plume migration.

V. DISCUSSION

Our experience using the SLFMR for field studies of Coastal Buoyancy Jets (CoJet) has demonstrated the utility and efficacy of L-band passive microwave mapping of sea surface salinity from an aircraft. It also points the way to future applications of similar technology deployed on earth orbiting satellites. In this work, we have focused on some challenges and new techniques for calibrating such radiometers, taking advantage of supporting in situ data. We have also presented preliminary results and interpretation of selected CoJet SSS maps. These illustrate the broad scope of possible applications of such technology. We now discuss these issues in more detail before considering overall system performance, ongoing developments and anticipated future advances.

A. Instrument Calibration

Calibration of L-band microwave radiometers for application to sea surface salinity mapping remains an active and challenging area of research. There are a number of reasons for this. The restriction to a protected 1.4 GHz band to minimize RFI and the corresponding wavelength of 21 cm effectively dictates antenna linear dimensions of order 1m, significantly larger than for S or C-band systems. This wavelength, coupled with the electrical properties of sea water, determines various characteristics of the radiometric measurement system. Examples include the depth of penetration (~ 5cm) in seawater, the response of emitted and reflected radiation to sea surface roughness elements and the range of influence of emitting or conductive structures in the near field. The latter include aircraft antennae, engine nacelles and superstructure that may affect the beam pattern and response. These are just a few of the environmental factors

that must be considered when calibrating L-band radiometers in the lab or field.

We have described two new methods for field calibration of an aircraft mounted L-band microwave salinity mapper, which account for the environmental influence of the physical temperature of the sea surface, aircraft attitude changes and atmospheric and extra-terrestrial (but not solar) radiation, and implicitly aircraft super structure. They can be applied in conjunction with lab calibration results or used as an independent validation of such results.

Our preliminary calibration method accounts for beam-to-beam brightness temperature offsets that may arise from errors in lab calibration or changes in hardware component characteristics that produce image striping artifacts in retrieved SSS maps. When applied in situations where the underlying assumptions are valid, the method gives results that compare well with the final calibration approach, given observed sampling and instrument noise levels. The method does not presently account for the effects of sea surface roughness. The development of algorithms for this purpose is presently an active area of research in the field that is making use of newly developed C-band radiometers to help estimate roughness effects on L-band response (section V-D).

B. Field Applications

During CoJet-III the SLFMR was used successfully to map a hypersaline body of water that develops during periods of low freshwater influx and high insolation, in shallow areas with restricted water circulation. The resulting maps demonstrate that airborne monitoring of seasonal changes in salinity ranging from fresh to saline (relative to standard seawater) is a practical possibility. The SLFMR is well suited to this application because of its large dynamic range (~5-400 K which may be compared with a range of ~80 – 140 K that could be expected from sea water even under extremely fresh or saline conditions). The hypersaline range is limited only by the presently validated range of the K&S algorithm (40 psu), but it appears that extensions to 45 psu or higher should be possible.

In its application to mapping the Cheseapeake Bay outflow plume, the versatility of the airborne mapping approach was demonstrated with repeated surveys at daily intervals that revealed quite dramatic changes in the location and extent of the associated coastal buoyancy jet that resulted from relaxation of down-welling favorable winds. Wind also played a significant role in determining the response of the Mobile Bay plume outside the confines of the Bay itself and adjoining Mississippi Sound. In contrast to the Cheseapeake Bay situation which illustrated a classic case of wind-driven coastal upwelling on a gently curving coast, the lower salinity water mass and wind influence extended of a significant portion of the continental shelf and within a more complex topographic setting. The more widely dispersed plume in this case made it difficult to attain complete coverage of the zone of influence of freshwater in a single day, and a split flight domain was employed. However, the new field calibration procedures should allow some of the resulting maps to be combined in a consistent manner, so that more complete coverage can be obtained.

The rapidity with which such surveys can be made exceeds that achievable using a research vessel while providing greatly enhanced spatial coverage. It must be recognized, however, that until laboratory and in-flight calibration techniques are improved to the point where they can be implemented simply, quickly and with sufficient accuracy, it appears that combined aircraft and ship operations will be needed to produce the necessary sea truth data for field calibration in the foreseeable future.

C. Instrument Performance

In spite of the challenges of retrospectively calibrating the SLFMR using field data, the survey examples presented show that the instrument performs remarkably well in its intended application to coastal sea surface salinity mapping. Repeated flights showed changes in SSS distribution that were consistent with in situ observations, independent of those used to calibrate the instrument. The instrument produced useful SSS distribution maps over a wide range of salinities from quite fresh to hypersaline. Frontal boundaries and other areas with large-scale spatial gradients were well represented and found to wax and wane or move in response to changes in observed meteorological and/or hydrological forcing.

D. Future Advances

A number of new developments will improve the accuracy and precision of microwave radiometers for mapping sea surfaced salinity from the air, and ultimately from space.

A new airborne instrument system, partly based on the SLFMR known as the Salinity, Temperature and Roughness Remote Scanner (STARRS) has recently been built for NRL by ProSensing Inc. [16]. This system combines, L-and C-band microwave radiometers with a dual head Infrared radiometer system to effectively observe surface conductivity, roughness and sea surface temperature simultaneously [5]. The L-band radiometer differs from that of the SLMFR in using Hach radiometer principles [21] in place of the Dicke Radiometer design [11]. In the new design the internal calibration process is implemented in software. This allows more control over instrument sensitivity and accuracy, since the sampling time for the target and internal references can be adjusted to optimize performance, with little or no impact on the hardware configuration. It utilizes the same 6-beam antenna configuration and beam-forming matrix approach as the SLFMR, but implements it using lighter and more compact patch antennae in place of dipoles. It also employs six identical radiometers, one dedicated to each channel; so it is a true multi-channel instrument. This allows simultaneous sampling on all channels to give a theoretical factor of 2.5 improvement in sensitivity. STARRS has recently been flown over the northern Gulf of Mexico (CoJet-IV) for sea surface roughness studies. It

was also employed by the European Space Agency to help test algorithms for a new satellite-borne instrument named SMOS, which stands for Soil Moisture and Ocean Salinity [22]. STARRS is currently being modified to further improve sensitivity and enable faster in flight calibration.

A new L and S-band radiometer system has recently been developed by NASA as a prototype for the Aquarius sea surface salinity satellite mission [23]. The instrument known as PALS [24] utilizes both passive and active microwave techniques and advanced designs to achieve improved stability and sensitivity. It has recently been used to extend the range of the K&S algorithm to 40 psu [19]. SMOS and Aquarius are both scheduled for launch in 2006, and this represents an excellent opportunity to extend the application of L-band radiometry to spanning the global oceans, while utilizing advanced airborne systems such as STARRS and PALS for smaller-scale surveys, algorithm development and ultimately find-scale tests of the performance of the satellite-borne systems.

VI. CONCLUSIONS

The application of L-band radiometers to mapping of Sea Surface Salinity in coastal domains including Florida Bay, Chesapeake Bay, and Mississippi Sound and adjoining continental shelf regions has been demonstrated. These domains were characterized by a wide range of salinity values and rapidly changing salinity distributions. New methods for field calibrating the instrument using in situ data, have also been presented and evaluated. These methods are seen as an essential adjunct to laboratory calibration now, and will remain so in the foreseeable future, until ultra-sensitive and stable radiometer designs are developed.

Continued advances in microwave radiometer design are expected to produce instruments with sufficient accuracy and precision to enable their use in mapping sea surface salinity distribution on a global scale within the next half-decade. We anticipate continued demand for in situ data to help monitor and improve performance of these satellite-borne systems. Efficient and more highly automated methods for calibrating the instruments both in the lab and in the field will be needed. Finally, advanced airborne systems will continue to provide the spatial resolution needed for fine-scale surveys of coastal buoyant plumes and fronts that cannot be resolved by foreseeable satellite instrument designs.

Acknowledgments

Mark Goodberlet, ProSensing Inc. built the SLFMR and actively participated in all aspects of its development. Collaborations with NOAA, which funded the development and loaned the instrument to NRL are gratefully acknowledged. NRL and the University of Southern Mississippi are thanked for financial support. Z. (Ken) Chen, Environmental Monitoring and Assessment Department, South Florida Water Management District actively participated in the Florida Bay work and provided the in situ data. Dr. R. Arnone, NRL provided the SeaWIFS satellite imagery.

REFERENCES

[1] D. M. Burrage, M. Goodberlet, and M. Heron, "Simulating passive microwave radiometer designs using SIMULINK," *Simulation*, Vol. 78 (1), pp. 36-55, Jan 2000.

[2] J. D. Droppleman and R. A. Mennella, "An airborne measurement of the salinity variations of the Mississippi River outflow." *J. Geophys. Res*., Vol. 75, 30, pp 5909-5913, 1970.

[3] J. L. Miller, M. A. Goodberlet, J. B. Zaitzeff "Remote sensing of salinity in the coastal zone," *EOS*, Trans. AGU Vol. 79, No. 14, April 7 pp. 3, 1998.

[4] J. L. Miller, "Airborne remote sensing of salinity," *Backscatter*, **11**, 3, 24-27, 2000.

[5] M. A. Goodberlet, C. T. Swift, K. P. Kiley, J. L. Miller, J. B. Zaitzeff, "Microwave remote sensing of coastal zone salinity," *J. of Coastal Res*., Vol. 13, No. 2, pp 363-372, 1977.

[6] A. Prytz, M.L.Heron, D.M.Burrage and M.Goodberlet "Calibration of the Scanning Low Frequency Microwave Radiometer," *Proceedings IEEE/MTS Marine Frontiers Oceans2002*, Biloxi, 29-31 Oct. 2002.

[7] M. L. Heron, D. M. Burrage and A. Prytz, "Terrigenous runoff in the tropics observed with a Scanning Low Frequency Microwave Radiometer," *Proceedings IEEE/MTS Marine Frontiers Oceans2002*, Biloxi, 29-31 Oct. 2002.

[8] D. M. Burrage, M. L. Heron, J. M. Hacker, T. C. Stieglitz, C. R. Steinberg and A. Prytz, "Evolution and dynamics of tropical river plumes in the Great Barrier Reef: An integrated remote sensing and in situ study," *J. Geophys. Res.,* Special issue on Salinity, 2002. in press.

[9] D. M. Burrage, J. L. Miller, M. A. Goodberlet and J. C. Wesson. "Features of coastal buoyancy jets observed with an airborne surface salinity mapper," presented at *AGU/ASLO Oceans2002*, Hawaii, Feb., 2002.

[10] Heron, M., D. Burrage and J. Hacker, "Sea surface salinity remote sensing campaign on the Great Barrier Reef," *Special Session on Sea Surface Salinity, Oceans from Space Symp*. 9-13 Oct., *In* Barale, J. et al., (eds.), *Ocean from Space, Venice 2000* IN EUR-19661 ERN p. 282, 2000.

[11] R. H. Dicke, "The measurement of thermal radiation at microwave frequencies," *The Review of Scientific Instruments*. Vol. 17, No. 7, pp 268-274, 1946.

[12] Ulaby, F. T., Moore R. K., Fung A. K., "Microwave remote sensing fundamentals and radiometery." . *Microwave Remote Sensing Active and Passive* Vol I pp 456, Artech House, Norwood, MA, 1981.

[13] Goodberlet, M.A., Swift C. T. "A Remote Sensing System for Measuring Estuarine and Coastal Ocean Surface Salinity," NOAA , Dept. Commerce SBIR Final Report, Contract 50-DKNA-1-00119, pp. 111, (Quadrant Engineering, Hadley, MA), Sept. 30, 1993.

[14] L. A. Klein, C. T. Swift "An Improved Model for the Dielectric Constant of Sea Water at Microwave Frequencies*," IEEE J. Oceanic Engr*., Vol. 2, No. 1, pp 104-111, 1977.
[15] M. Goodberlet and J. Miller, "NPOESS – Sea Surface Salinity," NOAA, Dept. Commerce Final Report Contract #43AANE704017, pp. 39, (Quadrant Engineering, Hadley, MA), 1997.
[16] M. A. Goodberlet, "Salinity Temperature and Roughness Remote Sensor (STARRS)," *Naval Research Laboratory-SSC Contract # N00173-00-C-6014 Final Report*, Jan. 3, 2001, pp. 35, ProSensing Inc., Amherst, MA.
[17] E. J. D'Sa, J. B. Zaitzeff, C. S. Yentsch, J. L. Miller and R. Ives, "Rapid remote assessments of salinity and ocean color in Florida Bay," In J. W. and K. G. Porter (eds) *The Everglades, Florida Bay, and Coral Reefs of the Florida Keys An Ecosystem Sourcebook* (CRC Press, LLC), pp. 451-459, 2002.
[18] Yates and Halley, http://sofia.usgs.gov/projects /circulation/data/sal_maps/]
[19] W. J. Wilson, S. H. Yueh, S. Dinardo and F. Li, "L/S-band radiometer measurements of a saltwater pond," (Jet Propulsion Laboratory, California Institute of Technology, Pasadena, CA, USA) unpublished.
[20] R. P. Stumpf, G. Gelfenbaum and J. R. Pennock "Wind and tidal forcing of a buoyant plume, Mobile Bay, Alabama" *Continental Shelf Research,* Vol. 13, No. 11, pp 1281-1301, 1993.
[21] J-P., Hach "A very sensitive airborne microwave radiometer using two reference temperatures," *IEEE Trans. on Microwave Theory and Techniques*, Vol. 16, No. 9, 629-636, Sept., 1968.
[22] Font, J., Y. Kerr, and M. Berger, Measuring ocean salinity from space. *Backscatter*, **11**, 3, 17-19, 2000.
[23] C. Koblinsky et al. "Aquarius Sea Surface Salinity: Understanding the response of the ocean to the global water cycle and climate," *Joint response to NASA Announcement of Opportunity 01-OES-01*, NASA GSFC & NASA JPL, July, 2001 pp. 20 + Appendices.
[24] W. J. Wilson, S. H. Yueh, S. J. Dinardo, S. Chazanoff, A. Kitiyakara, F. K. Li and . Rahmat-Samii, "Passive active L- and S-band (PALS) micrwave sensor for ocean salinity and soil moisture measurements," *IEEE Trans. Geosci. Remote Sensing,* Vol. 39, pp 1039-1048, May, 2001.